Equation-of-state studies using laser-driven shock wave propagation through layered foil targets

H. C. Pant[†,*], M. Shukla[†], V. K. Senecha[†], S. Bandyopadhyay[†], V. N. Rai[†], P. Khare[†], R. K. Bhat[†], B. K. Godwal[#] and N. K. Gupta[#]

[†]Laser Plasma Division, Centre for Advanced Technology, Indore 452 013, India
[#]High Pressure Physics Division, Bhabha Atomic Research Centre, Trombay, Mumbai 400 085, India

Results of laser-driven shock wave experiments for equation-of-state (EOS) studies of gold metal are presented. A Nd:YAG laser chain (2 Joule, 1.06 μm wavelength, 200 ps pulse FWHM) is used for generating shocks in the planar Al foils and Al + Au layered targets. EOS of gold in the pressure range of 9–13 Mbar is obtained using impedance-matching technique. Numerical simulations performed using one-dimensional radiation hydrodynamic code supports the experimental results. Experimental data show remarkable agreement with results from studies using the existing standard EOS models and with other experimental data obtained independently using laser-driven shock experiments.

STUDY of matter under extreme pressure conditions is a subject of great interest in several branches of physics, in particular, astrophysics, materials science and inertial confinement fusion research[1–3]. A proper knowledge of the equation-of-state (EOS) of materials at high pressures is the key requirement for such studies. EOS data[4,5] are also an important input to hydrodynamic codes used for the simulations of fission, fusion devices and their effects. Extensive data on materials have been generated using static and dynamic shock-wave techniques[6]. The range of such data using diamond-anvil cell and two-stage gas gun are limited to 5 and 10 Mbar pressures, respectively[5]. Theoretical treatment of materials in such compressed states is carried out using solid and liquid state theories[7]. The current state-of-the-art condensed matter models based on density functional theories, employing generalized gradient approximation for exchange and correlation potentials, have demonstrated their capabilities to predict phase transitions that, in turn, have been confirmed by experiments[7]. Remarkable agreement between theory and the state-of-the-art experiments has demonstrated beyond doubt that first-principle simulations can be carried out reliably to predict thermodynamic states of the materials up to 10 Mbars[8].

It is also well known that different variants of Thomas–Fermi–Dirac theory can be used to predict EOS data beyond 100 Mbar pressures[9]. However, the region of pressures from 10 to 100 Mbar is still not very well understood. This is mainly due to lack of sufficient experimental data in this region; till recently the experimental data were mainly from nuclear explosion experiments, which are difficult to perform[10]. Theoretical simulations in this region have been extremely difficult because of the complications arising from pressure and thermal ionization effects strongly controlled by atomic shell structure effects, which affect many physical properties along the shock Hugoniots of different materials[11]. Nevertheless, very few attempts based on first-principle theories have been made[12]. In order to test the predictions of such models and improve upon them, it is essential to have sufficient and accurate laboratory database.

Pressures higher than few tens of Mbars have been generated by high-power pulsed lasers[13]. In the past, pressures up to 100 Mbars were produced by shock waves generated in a solid target irradiated by a laser or in a target foil impacted by a laser-accelerated thin foil[14]. Such laser-driven shock waves, however, were not adequate for accurate EOS measurements because of large errors in the shock velocity measurements due to their spatial non-uniformity, variable shock pressures, and due to preheating of the material ahead of the shock front[15,16].

Recent laser-driven shock wave experiments have demonstrated high-quality planar shock waves induced by thermal radiation from hohlraum cavity with measured pressures as high as 750 Mbar[17,18]. However, in all such published work on laser-driven shock wave experiments, the pressure was determined indirectly from the measurement of the shock velocity and with the use of known EOS of a given reference material. Direct measurement of the EOS data requires simultaneous measurement of particle velocity also, as carried out in nuclear explosion-driven shock-wave experiments[19]. The work reported from Lawrence Livermore Laboratory has demonstrated the feasibility of such simultaneous measurements of shock and particle velocity using thermal X-ray drive, popularly known as indirect drive, obtained from primary laser-heated cavities[20]. In fact,

*For correspondence. (e-mail: hcp@cat.ernet.in)

EOS data in the few tens of Mbar pressure range have been obtained for low Z materials like SiO_2 and Be by measuring both the shock velocity and particle velocity[21]. Also, an intermediate route (between the conventional indirect method of pressure determination and the direct measurement) is known as the 'impedance-matching technique', involving measurement of shock velocity in two materials in stepped target configurations. This provided an opportunity to Koenig and coworkers[22] to test the relative consistency of the EOS of two materials, or, alternatively, for measuring EOS for one of the materials, using the EOS of the other material as a reference. By using the impedance-matching technique, the EOS of gold has been measured and is found to be consistent with the SESAME data up to 35 Mbar[23].

In the laser-plasma laboratory at the Centre for Advanced Technology (CAT), Indore, we are pursuing an experimental programme to study materials at extreme pressure conditions, created in the laboratory, using intense laser ablation-driven shocks. Such data on solid materials are very sparse and are obtained only through nuclear detonations. In order to obtain EOS data at high pressures using laser-induced ablation, efforts are being made to develop the technique for the measurement of the shock velocity in several materials. The present studies are carried out using a 2 Joule/200 ps laser at 1.06 μm wavelength. When focused, the intensity of the beam can reach up to 10^{14} W/cm^2. As described later in this paper, we have been able to establish the reliability of this technique that can be exploited for the measurement of EOS data of a variety of materials.

In this article, we also address the problem of measuring shock velocities in planar Al foil targets (reference material) and then use the impedance matching technique for shock velocity measurement through a test sample material deposited in a layer form at the rear surface of the reference material. We have used gold, as a sample material whose EOS is to be determined. We also describe the experimental arrangement used along with target preparation and characterization procedures. Next, we deal with the streak camera diagnostics for the unambiguous recording of laser-driven shock wave breakout signals and shock velocity measurements in a single foil target and a double layer foil target and details of Hugoniot determination. The predictions of numerical simulation results are also given, which help in proper understanding, interpretation and analysis of results. Results and discussion are followed by conclusions.

Experimental

An intense laser beam focused onto a thin solid target kept inside vacuum with initial density ρ_s (Figure 1 *a*) creates hot ablating plasma at the surface of the target. Laser energy is absorbed up to the critical density surface as shown in Figure 1 *b*. Plasma ablation in the early phase of laser pulse duration launches a compression wave in the target material due to momentum recoil. The successive compression waves generated by laser pulse after first compression in the initial phase, travel inside the compressed material at higher velocity than the first wave and develop a near discontinuous shock wave at approximately the peak of the laser pulse. The shock propagates into the target with shock velocity u_s and imparts a velocity u_p to the material behind the shock front. After the laser pulse is turned off, the ablation pressure and velocity begin to drop rapidly. At this time a rarefaction wave will set in and propagate from the ablation front into the shock compressed target. The ablation-driven shock wave propagates in the target material and heats the compressed material, thereby generating a visible optical emission when shock unloads at the rear surface of the target. The temperature and density profiles of the plasma at the target front surface along with shock wave discontinuity that is launched inside the target are shown in Figure 1 *b*.

A Nd:YAG cavity dumped-mode locked laser with a good spatial quality TEM_{00} output has been used as a driver. The laser electronics is modified to produce a single-shot operation[24]. An External Pulse Slicer (EPS) has been designed to improve the contrast ratio of the laser[25]. Two additional laser amplifiers make a Master Oscillator Power Amplifier (MOPA) laser chain to boost the energy from 180 mJ to 2 J range. The experimental arrangement is shown schematically in Figure 2. The intense picosecond laser pulse is focused on a planar solid target kept inside a vacuum chamber (pressure $\sim 10^{-3}$ bar) by a lens (focal length ~ 400 mm and diameter ~ 50 mm). The focal spot is measured to be ~ 100 μm and ~ 120 μm at two different focusing conditions. The high intensity ($\sim 10^{14}$ W/cm^2) created on the front surface of foil produces ablation of material that, in turn, launches a shock wave in the medium that generates intense thermal radiation on unloading at the rear surface. The hot emitting rear surface behaves like a black body and its luminescence emissivity signal is collected and focused by a lens on the entrance slit (width ~ 100 μm, length ~ 6 mm) of a visible (S-20) streak camera[26]. A CCD camera captures the streak-image, which is acquired in a personal computer (PC) through a frame grabber card for final image processing.

The optical streak camera that is used for detection of shock breakout signal has a temporal and spatial resolution of 20 ps and 100 μm, respectively. A fiducial signal is also recorded along with shock-induced luminescence by streak camera, each time the laser is fired on the target foil. It serves as a marker for the arrival of the laser pulse on the front surface of the foil. This has been

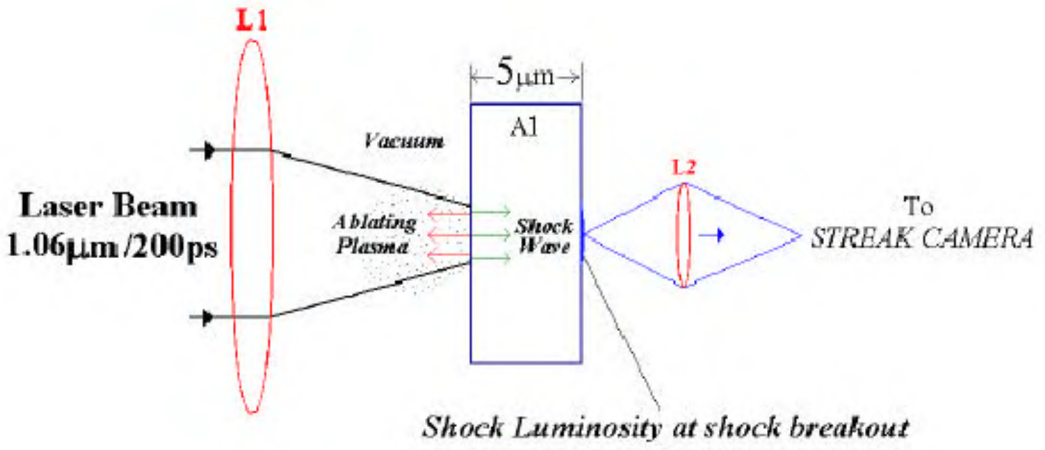

Figure 1 *a*, Illustration of laser-induced shock wave formation and shock luminosity.

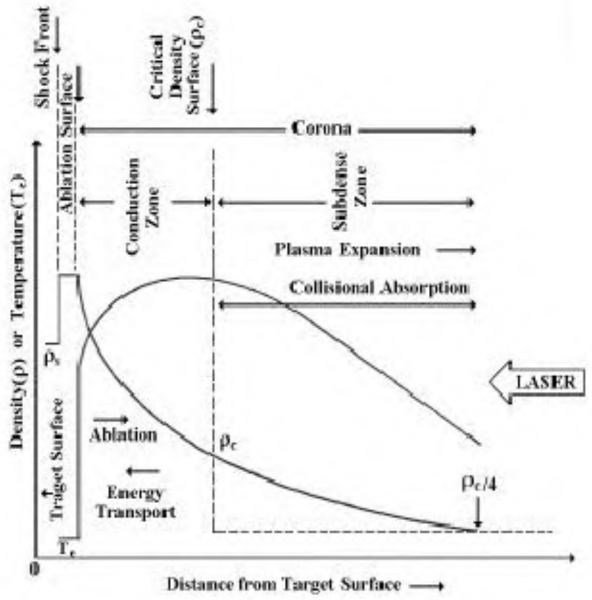

Figure 1 *b*, Density and temperature profiles of laser-produced plasma showing laser absorption up to critical density surface and shock compression.

achieved by picking up 4% laser reflections from a glass plate (wedge angle ~ 0.5°), placed before the focusing lens, and converting it to visible radiation by a second harmonic crystal of length 20 mm and then sending it along an optical fibre cable at the vertical slit input of the streak camera. In the slit, the fibre tip rests below the laser focal spot, where radiations from the target are expected to reach. This is confirmed by punching a hole in the foil by the Nd:YAG laser oscillator and then observing the position of a pre-aligned (with the YAG laser) He–Ne laser spot on the slit. The streak camera is triggered from a photo-diode that is also used to trigger the Pockel cell inside the laser cavity for cavity-dumping. The inherent electronics delay in the circuit is about 25 ns. In order to synchronize the streak operation with the arrival of the main laser pulse, the laser pulse is optically delayed by means of a pair of fully reflective mirrors (M_1 and M_2) before it is focused on a target. The arrival of laser-pulse at the streak input without any target material in the beam path is synchronized with the arrival of the fiducial signal by introducing an optical delay loop consisting of four fully-reflecting mirrors (M_3, M_4, M_5 and M_6) between the focusing lens and the beam-sampling glass plate (for fiducial arrangement) and adjusting the position of the beam sampler. With this set-up the delay in time between the shock arrival of induced luminescence signal and the fiducial signal gives the time the shock wave takes to traverse the target medium thickness. By knowing the foil thickness and measuring the time delay, the shock velocity can be calculated.

Shock velocity measurements and determination of pressure in standard reference material: Planar Al foils

We have prepared planar Al foil targets of different thicknesses by chemical etching process from an Al foil (density ~ 2.7 g/cm^3) of 12 μm thickness. Purified NaOH pellets (assay content ~ 97%) of Merck were dissolved in water and the solution was used to etch the foils. Each foil was first carefully fixed on a plexiglas frame in such a manner as to make the surface of the foil free. The assembly was then immersed in etching bath and held vertically during the operation. By controlling the etching time, foil thickness down to 3 μm was achieved. The foil thickness was measured by weighing the foil sample of a definite dimension (2.5 cm × 2.5 cm) in a microbalance. Target dimensions were chosen such that they satisfy the following criteria:

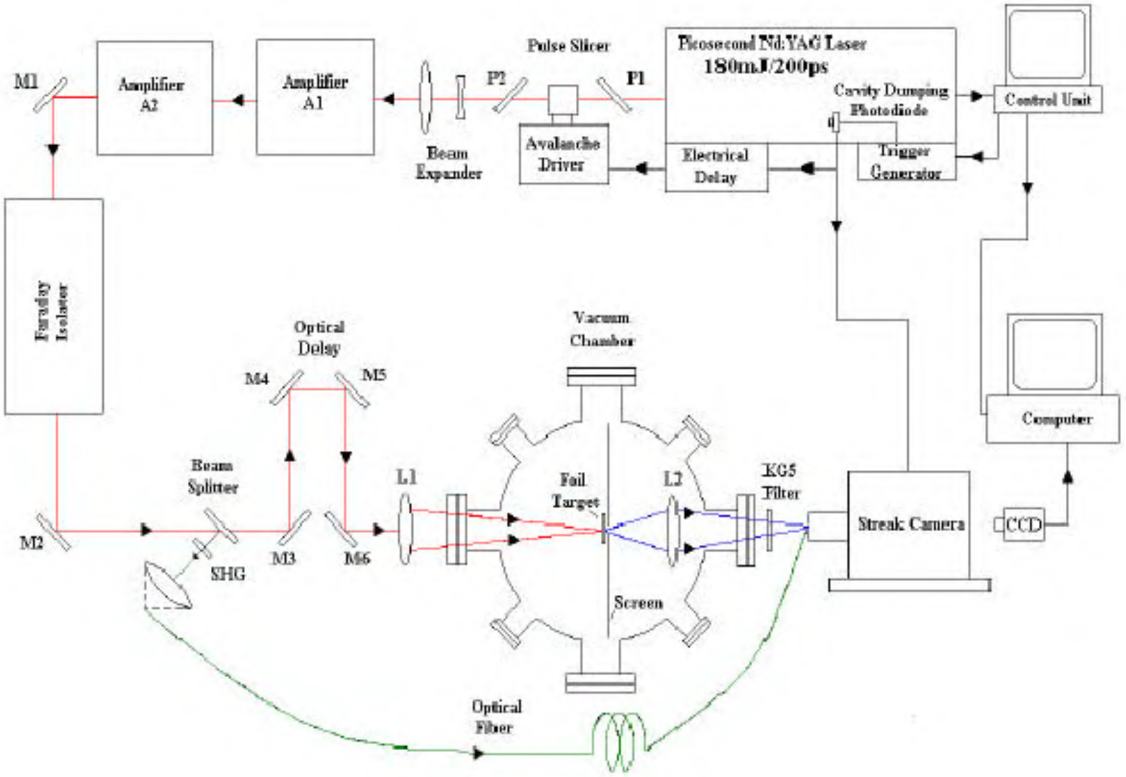

Figure 2. Schematic of the experimental set-up. M_1 , M_2, .. M_6 are fully reflecting mirrors; L_1 is focusing lens; L_2 is imaging lens.

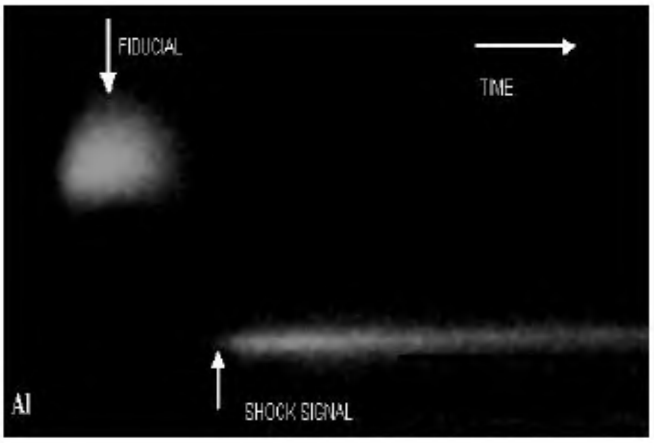

Figure 3. Typical streak camera record of a luminosity signal (picosecond resolution) captured through a CCD camera at the time of shock breakout from the rear surface of 5 μm thick Al foil.

a. Laser focal-spot diameter was small enough to produce the required high intensity, yet be much larger than the target thickness to minimize two-dimensional (2D) effects and hence ensure a planar shock[13].
b. The width of the target was much larger than the diameter of the laser focal spot to avoid the weakening of shock strength by edge rarefaction wave. This is also required to avoid the ablation plasma flow around the foil edges which otherwise disturbs the luminosity record.
c. After the termination of driving laser pulse, a rarefaction wave propagates at a speed higher than the shock wave and eventually overtakes and attenuates it. Therefore to ensure steady shock propagation (i.e. to avoid shock decay), the target thickness was chosen such that it satisfies the condition: $d \leq 2u_s\tau$, where d is target thickness, u_s is the shock velocity in the material and τ is the laser pulse length. Typical shock velocity in Al is ~10^6 cm/s and τ is 200 ps (FWHM of pulse)[27].
d. The thickness of the target was kept larger than the range of supra-thermal electrons and hard X-rays, to avoid pre-heat reaching ahead of the shock wave on the rear side of the target.

We have used planar Al foils (typically 3 to 4 mm wide) of thickness 3.17 μm, 4.64 μm, 5 μm and 8 μm. The shock breakout times for those targets were recorded at the same incident intensity of the laser beam. A typical experimental observation of shock emergence seen as strong luminosity, as recorded by streak camera is shown in Figure 3. One can notice the remarkably clean signal quality. The shock transit times were calculated with respect to the peak (centre) of the fiducial signal using image-processing software (PROMISE) developed in-house at CAT[28]. The time axis is calibrated by

counting the total number of pixels in the image plane of the full aperture of the phosphor screen and then comparing it with the time calculated from the known streak speed for a signal to sweep across the known diameter of the screen. The calibration factor was found to be 4.3 ps/pixel. The shock transit time (t) was found to be linear up to the foil thickness (d) of 6 μm. The average velocity was found by taking the inverse of the slope of the best linear fit to the data in the t–d plane. The results are presented in Figure 4 for absorbed laser intensity of $\sim 5 \times 10^{13}$ W/cm^2. Using a similar method, the shock velocity at absorbed laser intensity of $\sim 3 \times 10^{13}$ W/cm^2 was also obtained.

For calculation of the pressure and particle velocity corresponding to the experimentally found shock velocity in aluminium, the relationship between the shock velocity and the particle velocity, which is found to be linear for a wide range of pressures, was employed. According to the LASL databook[29] this can be written as:

$$u_s = 0.5386 + 1.339 u_p. \quad (1)$$

Velocity is in units of 10^6 cm/s. This relationship is used to calculate the particle velocity u_{p1} corresponding to the experimentally found shock velocity ($u_{s1} = 2.096 \times 10^6$ cm/s). The particle velocity thus determined is 1.163×10^6 cm/s. Once the values of both, the particle velocity and shock velocity are obtained, the pressure can be calculated from the standard Rankine–Hugoniot relationship:

$$P = \rho_0 u_s u_p, \quad (2)$$

where ρ_0 is the solid density (which is 2.7 g/cm^3 for Al and 19.24 g/cm^3 for Au). The pressure thus calculated is found to be 6.586 Mbar, which is the shock pressure induced in the aluminium foil.

Measurement of shock velocity in multi-layered targets and determination of gold Hugoniot data by impedance-matching technique

Deposition of 1.75 μm and 1.5 μm thick gold layers respectively, on the rear surface of Al foil of 5 μm thickness was carried out employing chemical and vacuum deposition techniques. The variation in thickness of 5 μm Al foil was of the order of ± 2%. A pressure of 10^{-5} bar was maintained in high-vacuum deposition system. Suitable changes were made in the process to obtain good adhesion and to keep variation in thickness within the specified range (± 0.2 μm).

The shock transit time was determined for two layer targets of 5 μm Al + 1.75 μm Au and 5 μm Al + 1.5 μm Au at absorbed laser intensities of 5×10^{13} W/cm^2 and 3×10^{13} W/cm^2, respectively. As the shock transit time for the reference material Al was known, the shock transit time for the gold layers was calculated. The shock velocities thus deduced were 1.19×10^6 and 1.02×10^6 cm/s respectively, for the above-mentioned laser intensities.

In the experiment, the target consists of Al foil as the base reference material and gold as a test material deposited on the rear surface. Since the density of Au is higher (~ 19.24 g/cm^3) compared to that of Al, its Hugoniot curve is located above that of Al. When shock arrives at the interface between the two materials, a shock wave is transmitted through Au and another one is reflected in the material Al. Experimentally we deduce the shock velocities u_{Al} (in Al) and u_{Au} (in Au) using the time difference in the shock luminosity signal recorded by the streak camera. As shown in the Figure 5, thick red and orange lines are the Rayleigh lines representing the final state (of adiabatically compressed material) attained with respect to an initial state on a pressure Hugoniot curve. Their slope values are $P_{Al} = \rho_{Al} u_{Al}$ and $P_{Au} = \rho_{Au} u_{Au}$ plotted in the (u, P) plane intersecting the Hugoniot curves (green lines) at (1.1635, 6.586) and (0.589, 13.468) points. Similarly, two other data points are represented as (0.927, 4.46) and (0.465, 9.01) on grey and black lines as Rayleigh lines. The reflected Hugoniot could be represented as H_1 ($2u_{p1}$–u_p), where H_1 (u_p) is the shock Hugoniot for Al and u_{p1} is the particle velocity induced by shock wave in Al. The intersection of the Rayleigh line with the reflected Hugoniot curve gives the EOS of gold. The final state determined this way as shown in Figure 5, gives pressure and the particle velocity in gold as 13.47 Mbar and 0.589×10^6 cm/s and 9.01 Mbar and 0.465×10^6 cm/s at absorbed laser intensities of 5×10^{13} W/cm^2 and 3×10^{13} W/cm^2, respectively.

Comparison with numerical simulations

Experimental measurements of shock velocity through layered targets can provide Hugoniot EOS data to a

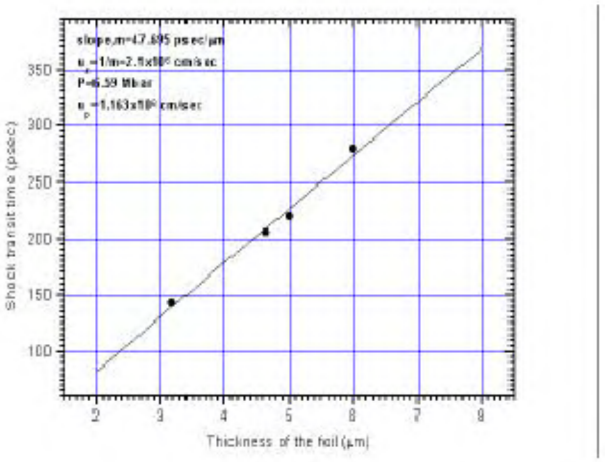

Figure 4. Shock transit time versus thickness of Al foil for shock velocity calculation.

fairly good accuracy ($\leq 10\%$)[30]. As mentioned earlier, we are using Al layer as a reference and Au as a sample material. During the experiment, we have ensured that the front side of Al and rear side of Au layers are fairly uniform in thickness, having surface smoothness $\pm 0.2\,\mu m$ over the sample area. In laser-driven shock wave experiments aimed at accurate measurements of EOS of any unknown material, it is essential to ensure that planar shock wave-fronts propagate in a steady-state condition through the reference material as well as through the test sample material. This requires a proper choice of target thickness. In case of very thin targets, the shock breakout occurs much earlier to the laser-driver pulse peak time. This leads to unsteady shock wave propagation through the target, because shock waves are in the acceleration phase. On the other hand, rarefaction wave from the laser irradiation side can interact with the shock wave for a very thick target. It also leads to non-uniform shock. Therefore, proper radiation hydrodynamic simulations can serve as an important tool in predicting proper target thickness that can avoid the effects of preheating and also ensure steady-state shock-wave propagation conditions. In the present experiments where we use thin Al foil targets of varying thickness, we have carried out a detailed one-dimensional (1D) numerical simulation study using radiation hydro code MULTI[31]. The code uses a multi-group method of radiation transport coupled with Lagrangian hydrodynamics based on fully implicit numerical scheme. Material properties like EOS, Planck and Rosseland opacities and non-LTE properties (for gold) are used in tabulated form, which are generated externally. This code has already been successfully used in analysing and interpreting several important experimental results related to laser-produced plasmas[32,33]. In the context of EOS studies also, this code has been extensively used in predicting and interpreting several experimental results[15,24,34]. Two-dimensional effects in our case will be insignificant, as target thickness (typically 3.4–6 μm) is much smaller than the focal spot diameter of 100–120 μm. Simulation results show that for the experimental laser irradiation ($I = 5 \times 10^{13}$ W/cm^2; $\lambda = 1.06\,\mu m$; pulse FWHM = 200 ps), the base material must be thicker than 3.4 μm to reach stationary condition. The results of computer simulation give the density profile for 5 μm shocked Al at 5×10^{13} W/cm^2 absorbed laser irradiance. The density profile gives a shock velocity of 2.08×10^6 cm/s. It is found to be quite consistent with the experimental value of 2.09×10^6 cm/s. We also noticed that the shock wave front reaches a steady-state condition at 250 ps after the start of the laser pulse and it continued in this state till it breaks out from the rear surface at 300 ps. Similarly, the pressure profiles also indicate steady shock pressure conditions attained at 250 ps after the start of the laser pulse and shock breakout at 300 ps. The temperature profiles obtained for the above case revealed that near the corona region its value was about 1 keV and the thermal wave propagates in the inner layers of the target, with temperature falling substantially at the time of shock breakout. The rear-side temperature was found to be about 0.2 eV before the shock breakout, which rules out the possibility of any X-ray preheat signal arriving before the shock front. The moment the shock breaks out, the temperature increases to about 1.5 eV. This is in conformity with the spectral sensitivity of S-20 photo cathode of the streak camera. Higher temperature at the rear side is noticed in thin targets of 1 to 2.5 μm thickness, where X-ray preheat leads to higher rear-surface temperature before the shock breakout. The shock pressure profiles obtained through simulations are shown in Figure 6. They give a peak pressure value of around 7.5 Mbar at $\sim 5 \times 10^{13}$ W/cm^2 absorbed laser intensity. This is about 10% higher compared to the pressure value obtained experimentally. This value is very closely related to the laser energy absorption. Thus the laser absorption coefficient is a crucial parameter to be used in the numerical simulations. Also non-LTE transport in corona region has to be considered.

We have also performed simulations for a multi-layer (Al + Au) target. The target and laser specifications are according to our experimental conditions. Simulation results illustrated in the Figure 7 show that for layered targets (Al + Au), the shock pressure gets enhanced by nearly a factor of 2 at the boundary of the two materials. Our experimental result also gives similar pressure enhancement in the Al + Au (5 + 1.75 μm) target, due to impedance matching at the boundary of the two materials. The numerical simulation results presented here support the steady shock-wave propagation through a given target thickness range used in the present experiments.

Results and discussion

We have compared experimental data for the shock velocity in aluminum and in gold with the SESAME data[35,36]. The Hugoniot curve for gold from experimental data also shows remarkable agreement with the theoretical data available in LASL data book or SESAME data. The relationship between the shock velocity and the particle velocity for gold can be expressed as:

$$u_s = a + b u_p,$$

Here a and b are constants. The published data from LASL gives (a, b) = (0.312, 1.1521). This compares well with our experimental values of (0.312, 1.488) and (0.312, 1.495) at absorbed laser intensities of 5×10^{13} W/cm^2 and 3×10^{13} W/cm^2, respectively. By extrapolating our Hugoniot curve to lower pressures and

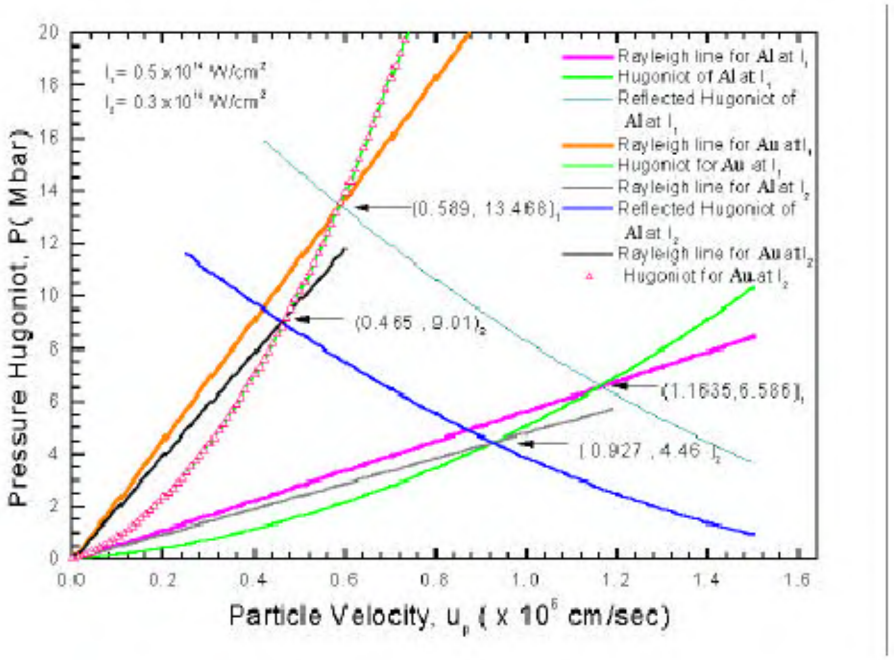

Figure 5. Experimental determination of pressure and particle velocities in Au material of a layered Al + Au target using impedance-matching technique. The pressure and particle velocity are continuous at the interface. Thus the point (0.465, 9.01) is located at the intersection of the Hugoniot curve of Au (green curve with red Δ symbols) arising from the initial state ($u = 0$, $P = 0$), with reflected shock Hugoniot (thick blue curve) of Al arising from point (0.927, 4.46). Similarly, for the second data point (1.1635, 6.586) on Al Hugoniot curve (green line) we obtain the data point (0.589, 13.468) by intersection of Au Hugoniot curve with the reflected shock Hugoniot (thin blue curve) curve. The grey and red lines are the Rayleigh lines meeting the Al Hugoniot curve at two points and their slope is equal to the product of solid density and shock velocity. Similarly, the black and orange lines are the Rayleigh lines on Au Hugoniot curve with slope equal to the product of solid density and shock velocity.

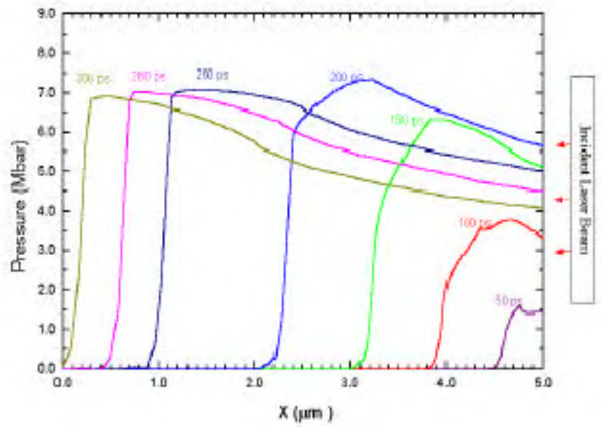

Figure 6. Pressure profiles of Al foil target (5 μm) irradiated with ps laser beam (2 J, 1.06 μm, 200 ps pulse FWHM) are generated using one-dimensional numerical simulations performed using MULTI code. The *X*-axis here represents the Eulerian coordinates showing position of the shock fronts at different time steps when the plasma is heated and is expanding. One can see the steady shock-wave propagation starting immediately after the peak of the laser pulse (200 ps) and continuing till shock breaks out from the rear surface.

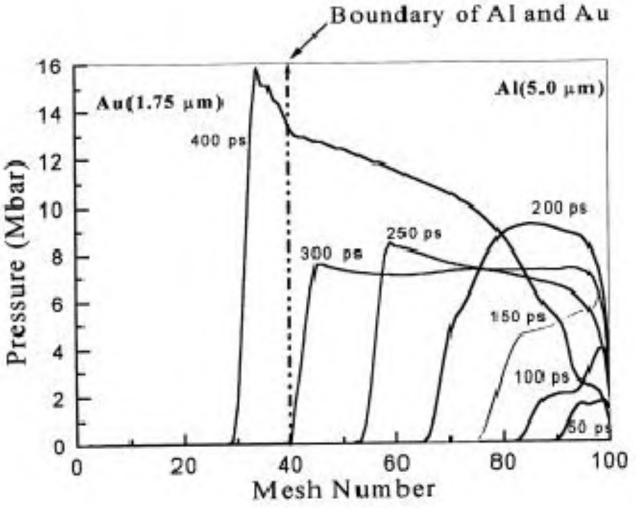

Figure 7. Pressure profiles for Al + Au targets are plotted against the mesh number (1–40 mesh corresponding to 1.75 μm thickness of Au layer and 41–100 mesh corresponding to Al base material). One can clearly observe the pressure enhancement by a factor of ~ 2 near the boundary of the two materials.

computing the volume compression, we have compared our data with those simulated by Godwal and Jeanloz[37]. Figure 8 shows that the simulated results are in good agreement with data from other laboratories. The published work of Jones *et al.*[38] and the data from indirect drive HELEN laser (AWE, UK)[30] experiments are also

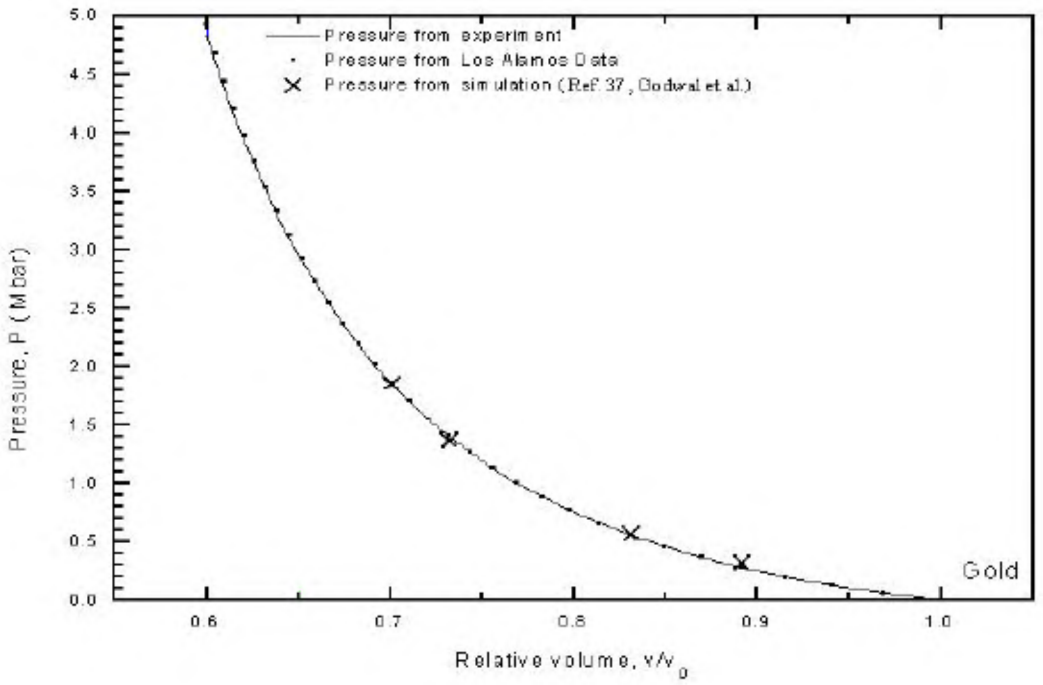

Figure 8. Experimental data points of pressure in gold are plotted against relative volume. When extrapolated to low-pressure regime, it shows excellent matching with the Los Alamos data and simulation data obtained by Godwal and Jeanloz[37].

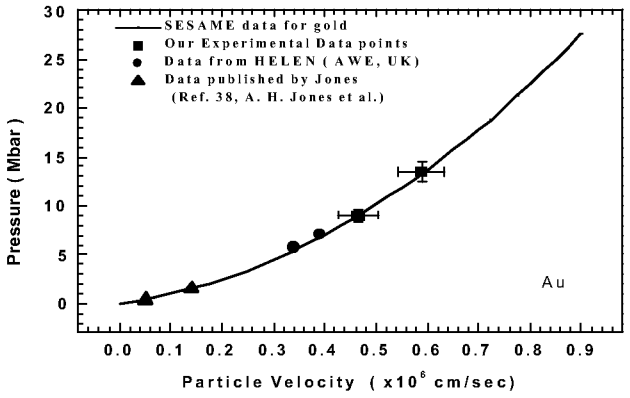

Figure 9. Present experimental EOS Hugoniot points for gold (shown with solid squares) and other previous experimental data points (solid circles and solid triangles) show good agreement with the SESAME curve.

presented, along with our results in Figure 9. The experimental pressure multiplication ($m = P_{Au}/P_{Al}$) factor of 2 at the interface of Al and Au materials is in close agreement with the theoretically predicted formulations.

From the comparison of experimental results with simulation results, we can say with confidence that our shock velocity measurements and Hugoniot EOS points are in fairly good agreement within the shock transit time error of about 5% and within the error of 2% in target thickness measurements. Thus our shock pressure values determined in the present experiments are correct within an error of 15–18%. In order to achieve a high level of accuracy (± 10% in pressure), the error in shock velocity measurements should be kept within ± 5%. This requires use of direct drive method after optical smoothing of laser-driver beam using random phase plates or phase zone plates. As a good alternate to the above technique, an indirect drive method alleviates the problem of laser intensity modulations. In the present experiment, where we are not working in very high intensity zone, no attempt was made to achieve a flat spatial beam profile. However, special care was taken in removing any pre-pulse present in the laser beam and a smooth Gaussian laser beam was maintained.

The experimentally determined shock pressure and velocity values are in good agreement with theoretical simulations. The scaling law for the variation of ablation pressure (P) with intensity (I) of the laser light is observed to be P (Mbar) $\sim (I/10^{14}\ \mathrm{W/cm^2})^{0.765}$ for aluminum and P (Mbar) $\sim (I/10^{14}\ \mathrm{W/cm^2})^{0.787}$ for gold. These results are in good agreement with published data from other laboratories[39,40]. Further, the improvement in target fabrication and characterization, streak camera calibration and data analysis with planarity of shock front are essential. Still the removal of pre-pulse and smooth laser pulse profile obtained in our laser chain has helped in obtaining the Hugoniot EOS data points to a fairly good accuracy. However, for future EOS measurement studies at even higher laser intensities, we are

attempting to use random phase plate and Fresnel zone plates, to ensure flat spatial beam profiles.

Conclusions

We have shown the feasibility of using a simple laser-driven system (Nd:YAG, 2 Joule, 1.06 μm, 200 ps) for conducting shock-wave experiments for EOS measurements of gold in thin-layered targets at moderate pressures of 9–13 Mbar range. A fast streak camera system coupled with a fibre-based fiducial signal marker records the shock breakout times. The results are quite consistent with theoretical as well as experimental data published by other laboratories. Impedance matching technique was successfully used to find the pressure in gold in a multilayer (Al + Au) target. A simple technique has been presented to find the Hugoniot curve of gold at 9 and 13 Mbar pressures. The laser-driven shock velocities and particle velocities obtained for gold are in excellent agreement with the reported results of other laboratories, including the SESAME data from the Los Alamos laboratory. The pressure amplification factor of 2 has been derived in Al + Au layered targets using MULTI group hydrodynamic simulations and the experimental results are in close agreement with results from numerical simulations.

1. Lindl, J., *Phys. Plasmas*, 1995, **2**, 3933–4024.
2. Celliers, P. M. *et al.*, *Phys. Rev. Lett.*, 2000, **84**, 5564–5567; Nellis, W. J., *Sci. Am.*, 2000, 60–66.
3. Remington, B. A., Drake, R. P. and Arnett, D., *Phys. Plasmas*, 2000, **7**, 1641–1652.
4. Chidambaram, R., *J. Indian Inst. Sci.*, 1996, **76**, 437–457.
5. Sikka, S. K. *et al.*, *High Pressure Shock Compression of Condensed Matter* (eds Davison and Sahinpoor), Springer Verlag, New York, 1997, p. 1.
6. Godwal, B. K., Sikka, S. K. and Chidambaram, R., *Phys. Rep.*, 1983, **102**, 121–171.
7. Godwal, B. K., Nag, A. and Da Silva, L. B., *Phys. Lett. A*, 1990, **144**, 26–29.
8. Godwal, B. K. *et al.*, *Advances in High Pressure Research in Condensed Matter* (eds Sikka, S. K. *et al.*), NISCOM, New Delhi, 1997, p. 45.
9. Zharkov, V. N. and Kalinin, V. A., in *EOS for Solids at High Pressure and Temperatures*, Consultants Bureau, New York, 1971, p. 1.
10. Ragan, C. E. III, *Phys. Rev. A*, 1984, **29**, 1391–1402.
11. Godwal, B. K. *et al.*, *Phys. Rev. Lett.*, 1981, **47**, 1144–1147.
12. Ross, M., *Phys. Rev. B*, 1980, **21**, 3140–3152.
13. Trainor, R. J. *et al.*, *Phys. Rev. Lett.*, 1979, **42**, 1154–1157, and references therein.
14. Cottet, F. *et al.*, *Appl. Phys. Lett.*, 1985, **47**, 678–682; Faral, B. *et al.*, *Phys. Fluids B*, 1990, **2**, 371–378.
15. Benuzzi, *et al.*, *Phys. Plasmas*, 1998, **5**, 2410–2420.
16. Honrubia, J. J. *et al.*, *Laser Part. Beams*, 1998, **16**, 13–20.
17. Cauble, R. *et al.*, *Phys. Rev. Lett.*, 1993, **70**, 2102–2105.
18. Lower, Th. *et al.*, *Phys. Rev. Lett.*, 1994, **72**, 3186–3189.
19. Volkov, A. P. *et al.*, *JETP Lett.*, 1980, **31**, 588–592.
20. Hammel, B. A. *et al.*, *Phys. Fluids B*, 1993, **5**, 2259–2264.
21. Da Silva, L. B. *et al.*, *Phys. Rev. Lett.*, 1997, **78**, 483–486.
22. Koenig, M. *et al. Phys. Rev. Lett.*, 1995, **74**, 2260–2263.
23. Batani, D. *et al.*, *Phys. Rev. B*, 2000, **61**, 9287–9294.
24. Shukla, M. *et al.*, Proceedings of National Symposium, Hyderabad, 1999, 61–62.
25. Bandyopadhyay, S. *et al.*, Proceedings of National Symposium, Hyderabad, 1999, 21–22.
26. Rai, V. N., Shukla, M., Pant, H. C. and Bhawalkar, D. D., *Sādhanā*, 1995, **20**, 937–954.
27. Gu, Y. *et al.*, *Laser Part. Beams*, 1996, **14**, 157–169.
28. Vora, H. S. *et al.*, CAT Report, CAT/1996/10, 1996.
29. Marsh, S. P. (ed.), *LASL Shock Hugoniot Data*, University of California Press, 1980.
30. Evans, A. M. *et al.*, *Laser Part. Beams*, 1996, **14**, 113–123.
31. Ramis, R. *et al.*, *Comp. Phys. Commun.*, 1988, **49**, 475–500.
32. Gupta, N. K. *et al.*, *Laser Part. Beams*, 1995, **13**, 389–395.
33. Eidmann, K. *et al.*, *Laser Part. Beams*, 1991, **9**, 551–560.
34. Senecha, V. K. *et al.*, *J. Phys. Condensed Matter*, 2001, in press.
35. Bennet, B. T. *et al.*, LANL Report, 1978, LA–7130.
36. Batani, D. *et al.*, *Laser Part. Beams*, 1996, **14**, 211–223.
37. Godwal, B. K. and Jeanloz, R., *Phys. Rev. B*, 1989, **40**, 7501–7507.
38. Jones, A. H. *et al.*, *J. Appl. Phys.*, 1966, **37**, 3493–3497.
39. Salzmann, D. *et al.*, *Phys. Rev. A*, 1983, **28**, 1738–1751.
40. Grun, J., NRL Memorandum Report, 1981, No. 4491, pp. 52–86.

ACKNOWLEDGEMENTS. We acknowledge the encouragement and support received from Dr Anil Kakodkar. We are extremely grateful to Dr R. Chidambaram for his keen interest in the work and Dr D. D. Bhawalkar for his constant support and help. We are also indebted to Dr S. K. Sikka for the fruitful discussions and many helpful suggestions. Dr S. N. Vyas and his colleagues are acknowledged for their help in target fabrication and characterization. Members of high-power glass laser and electronics group deserve our special thanks for their technical help and support during the experiment and at various stages of the laser chain development.

Received 17 July 2001; revised accepted 6 November 2001